Annals of Biomedical Engineering, Vol. 26, pp. 128–137, 1998

0090-6964/98 $10.50 + .00

Estimation of Organ Transport Function from Recirculating Indicator Dilution Curves

GIOVANNI SPARACINO,* RICCARDO BONADONNA,† HELMUT STEINBERG,‡ ALAIN BARON,‡ and CLAUDIO COBELLI*

*Department of Electronics and Informatics, University of Padova, Italy, †Division of Endocrinology and Metabolic Diseases, Azienda Ospedaliera di Verona and University of Verona Medical School, Verona, Italy, and ‡Richard Roudebush Veterans Affair Medical Center, Department of Medicine, Indiana University, Indianapolis, IN

(Received 22 July 1996; accepted 16 June 1997)

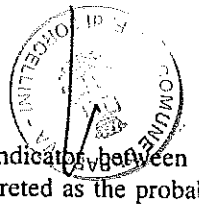

Abstract—The transport function of an indicator through an organ allows the calculation of important physiological parameters, but its estimation, especially in the presence of recirculation, can be difficult. In this paper, we estimate the transport function of ^{3}H-mannitol (an extracellular tracer of glucose) in the human leg skeletal muscle. To do so, an indicator bolus is administered into the femoral artery and its recirculating dilution curves are nonuniformly sampled in both the femoral artery and the femoral vein. A new deconvolution-based method is used to simultaneously estimate the indicator transport function and the organ plasma flow. Subsequently, the indicator mean transit time and distribution volume are calculated. The reliability of the method is assessed by Monte Carlo simulation. The ability to estimate parameters, like mean transit time and extracellular distribution volume, is critical to the study of pathophysiologic states such as diabetes, insulin resistance, and hypertension. © *1998 Biomedical Engineering Society.* [S0090-6964(98)01001-7]

Keywords—Mannitol, Deconvolution, Mathematical model.

INTRODUCTION

An indicator dilution curve (IDC) at the inlet of an organ, say $u(t)$, can be put in relation, assuming the system linear and time invariant, with the concentration of the same indicator at the outlet of the organ, say $z(t)$, by the convolution integral

$$z(t)=\int_0^t h(t-\tau)u(\tau)d\tau=\int_0^t u(t-\tau)h(\tau)d\tau, \quad (1)$$

where $t=0$ is the time of the indicator administration. The function $h(t)$ is the impulse response of the system, i.e., the output of the system when the input is a Dirac pulse. If there is no loss of the indicator between the input and output, $h(t)$ can be interpreted as the probability density of the transit times through the organ from inlet to outlet[19] and is called the transport function of the indicator through the organ.

The knowledge of the transport function $h(t)$ is essential to compute important physiological parameters. For instance, the mean transit time (MTT), i.e., the average time a particle of the indicator spends in the organ before exiting it, and the distribution volume (V) can be calculated, respectively, as

$$\text{MTT}=\int_0^\infty th(t)dt, \quad (2)$$

$$V=F\text{MTT}, \quad (3)$$

where F is the organ plasma flow.

If no recirculation is present, the estimation of $h(t)$ is straightforward if a bolus injection of a tracer mass D is administered in the organ inlet in a time shorter than the minimum system transit time. Under this hypothesis, the bolus injection is equivalent, for the system described by Eq. (1), to a pulse input $u(t)=U_0\delta(t)$, where U_0 is the amplitude of the concentration pulse, related to D by $U_0=D/F$. The output IDC is, thus, $z(t)=U_0h(t)$, a curve which typically exhibits a sharp increase with an unimodal peak and a slow decrease. The plasma flow F can be obtained by dividing the indicator mass D by the area under $z(t)$.[6,19] Then, having obtained U_0, $h(t)$ is calculated from $z(t)$.

Often, however, there is a significant recirculation of the indicator, i.e., a particle exiting the organ returns to the inlet and acts as input again. This is, for instance, the case of the indicator examined in this work, where a bolus of ^{3}H-mannitol, an *extracellular* tracer of glucose, is injected into the femoral artery but a significant fraction of it appearing in the femoral vein returns to the

Address correspondence to Professor Claudio Cobelli, Department of Electronics and Informatics, University of Padova, Via Gradenigo 6/A, 35122 Padova, Italy. Electronic mail: cobelli@dei.unipd.it

Giovanni Sparacino is presently with the Department of Audiology and Phoniatrics, University of Padova and Azienda Ospedaliera di Padova, Padova, Italy.

artery because of recirculation. As a result, a smooth inlet IDC is generated and both $z(t)$ and $u(t)$ exhibit very long tails. In the recirculation case, the estimation of $h(t)$ is difficult and requires, first, to monitor both the outlet and inlet IDC, and then a method to determine $h(t)$ from $u(t)$ and $z(t)$ exploiting the convolution integral.[1] Of note is that a similar necessity also arises when the injection occurs at a point upstream from the organ inlet so that $u(t)$ is a somewhat skewed pulse and the shape of the measurable output $z(t)$ no more coincides with that of the unknown $h(t)$, e.g., Ref. 17.

The most natural way to attack this kind of problem is deconvolution. Deconvolution can be parametric or nonparametric. Parametric deconvolution assumes *a priori* the functional form of $h(t)$, and this usually makes it highly problem oriented. On the other hand, nonparametric deconvolution is in general difficult because of ill conditioning. For instance, the tail of the estimated transport function can exhibit artifactual oscillations, thus, producing unreliable estimates of MTT. Moreover, nonparametric methods cannot provide estimates beyond the period of data collection, and this can affect the possibility of evaluating Eq. (2) correctly. Here, in addition, since the ^{3}H-mannitol bolus is administered at the inlet of the organ, where a large but unknown plasma flow occurs, the input IDC also depends on an unknown quantity and deconvolution cannot be performed. There is, thus, the need to simultaneously estimate $h(t)$ and F from the recirculating artery and vein IDC.

In this paper, the problem is approached by a recently developed nonparametric deconvolution method coupled with a suitably designed modeling procedure, which extrapolates the tail of the transport function up to infinity. The method is applied to ^{3}H-mannitol data obtained in the leg skeletal muscle of normal subjects, the final aim of the experiments being to provide a measure of the extracellular distribution volume. This parameter is physiologically important because evidence is accumulating to suggest that insulin stimulation is associated with an increase in the extravascular space by virtue of an increase in tissue recruitment,[4,23] and that pathophysiologic states such as diabetes, insulin resistance, and hypertension may be associated with a reduced insulin effect at that level.[1,4,18] The accuracy and precision of the method are assessed by a Monte Carlo strategy.

EXPERIMENTAL PROTOCOL AND DATABASE

Twelve healthy volunteers were studied at the Indiana University General Clinical Research Center, Indianapolis, IN. All subjects were studied after an overnight fast in the supine position. At 7.00 a.m., a catheter was inserted into the antecubital vein for infusion of substances. Subsequently, the right femoral artery and vein were cannulated. A 5 French sheath with side arm (Cordis Corporation, Miami, FL) was placed in the right femoral vein to obtain venous blood. The right femoral artery was cannulated with a 5.5 French double lumen catheter (Arrow International, Reading, PA) to allow for injection of the tracer through the proximal port (most caudad) and withdrawal through the distal port (most cephalad). An average dose of 2.2×10^8 dpm of ^{3}H-mannitol (New England Nuclear Research Products, Wilmington, DE) was administered at time zero into the femoral artery in about 1.5 s. Plasma samples were collected for 45 min, say, the experiment duration D_e, from both the femoral artery and the femoral vein on a non-uniformly spaced grid. The sampling period ranged from 0.2 to 3 min. Let us denote by Ω_{sv} and Ω_{sa} the vein and the artery sampling grids, respectively. A typical Ω_{sv} is: 0.2 0.4, 0.6, 0.8, 1, 1.2, 1.4, 1.6, 1.8, 2, 2.4, 2.8, 3.2, 3.4, 3.8, 4.2, 4.6, 5, 5.5, 6, 6.5, 7, 7.5, 8, 8.5, 9, 10, 11, 12, 13, 14, 15, 16, 17, 18, 20, 22, 24, 26, 28, 30, 33, 36, 39, 42, and 45. On the average, Ω_{sa} is similar to Ω_{sv}: it has the same duration of Ω_{sv} but it can be slightly sparser than Ω_{sv} in the first 20 min. The sampling schedules reflect the expected changes in the IDCs, i.e., the samples are collected more frequently where the variations of the signals are expected to be faster. The protocol was subsequently repeated in four of the 12 subjects to assess reproducibility.

^{3}H-mannitol counts were determined in the femoral artery and vein serum obtained by aliquoting it into 200 μl samples. 300 μl of perchlorate were added to the aliquot, vortexed, and spun at 2500 rpm for 20 min. 250 μl aliquots of the supernatant were pipetted off and placed into a scintillation vial and allowed to dry with 5 ml of scintillation fluid. Once dry, the remnant was resuspensed with 250 μl of distilled water, and 5 ml of scintillation fluid were added (Ecoscint Scintillation Fluid, National Diagnostics, Atlanta, GA) for the determination of total ^{3}H-dpm on a tricarb liquid scintillation analyzer (model 2100TR, Packard Instruments Company, Meriden, CT).

Measurement error variance of tracer data was obtained by summing the variance of the radioactivity and the variance of the pipetting errors (independently assessed in the laboratory). The coefficient of variation (CV) resulted approximately constant and around 6%. Measurement errors were assumed additive, independent, and normal.

A representative artery and vein IDC (subject No. 4) is shown in Fig. 1. Note that, since a large (but unknown) plasma flow is present, sampling at the input site does not allow tracing the "original" input pulse in the artery IDC; the only samples of the input IDC, which can be provided are those due to recirculation. The vein IDC decays to zero very slowly: its duration reflects the duration of both the recirculating input IDC and the impulse response.

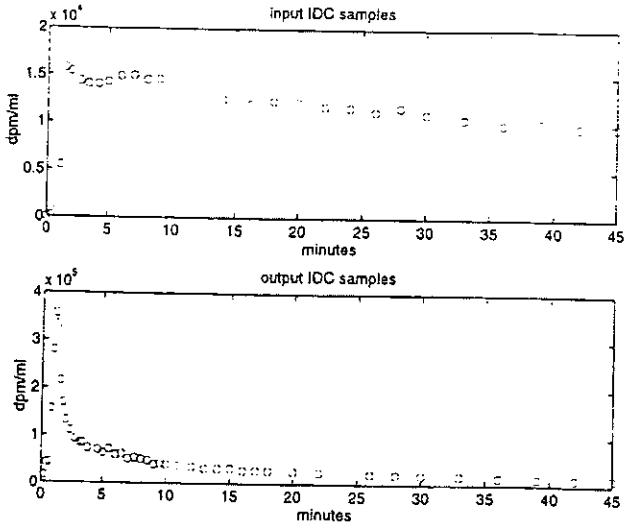

FIGURE 1. A representative data set (subject No. 4). *Top.* Samples of the recirculating artery IDC. *Bottom.* Samples of the vein IDC.

METHODOLOGY

The Strategy

The input $u(t)$ of the system we are considering consists of two components: the "original" pulse, i.e., the administered tracer bolus, and the "recirculation" input, i.e., the smooth contribution originated by the tracer, which returns to the organ inlet. Figure 2 displays a block diagram of the system, where the signal over the arrow exiting a block (output) is causally related to the signal over the arrow entering the same block (input): the recirculating inlet IDC is viewed as the effect of a positive feedback. The system input $u(t)$ is thus modeled as

$$u(t)=\frac{D}{F}\,\delta(t)+u^R(t), \tag{4}$$

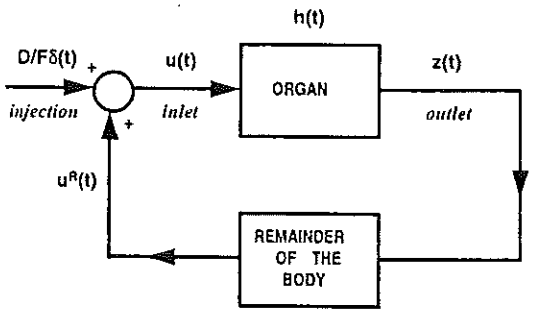

FIGURE 2. Block diagram of the system. The signal over the arrow exiting a block (output) is causally related to the signal over the arrow entering the same block (input). The circle denotes a signals adder.

where D is the (known) bolus mass, F is the (unknown) plasma flow through the organ, and $\delta(t)$ denotes the Dirac pulse. Samples of $u^R(t)$ are measured in the femoral artery. Note that the Dirac function approximation of the input used in Eq. (4) is realistic only if the duration of the tracer injection is less than the minimum system transit time.

Our goal is to estimate $h(t)$ from the sampled input, i.e., $u(t)$ on Ω_{sa}, and output, i.e., $z(t)$ on Ω_{sv}, IDCs. However, deconvolution in Eq. (1) cannot be done in a straightforward manner because the input IDC, given by Eq. (4), depends on an unknown parameter, the plasma flow F.

To proceed, we have exploited the physiological information that no loss of indicator occurs between the organ inlet and outlet. In mathematical terms, this *a priori* knowledge translates into the statement that a "consistent" estimate of $h(t)$, say $\hat{h}(t)$, must satisfy

$$\int_0^\infty \hat{h}(\tau)d\tau=1. \tag{5}$$

The physical constraint given by Eq. (5) has suggested to us the following strategy: (1) Assume a trial value for F in Eq. (4); (2) provide, by a deconvolution-based method, an estimate $\hat{h}(t)$, of the transport function for $0\leqslant t<\infty$; and (3) compute the left side of Eq. (5): if the estimate does not satisfy Eq. (5), select a different trial value of F and repeat step (2). The core of this strategy is the estimation of $h(t)$, which is discussed below.

Estimation of the Transport Function

State of the Art. For the estimation of the transport function by deconvolution, the literature has often resorted to parametric methods. Roughly speaking, in parametric methods, the transport function is given *a priori* a known functional form, usually depending on a small number of unknown parameters, which are fitted against the data.[2,13,16,17,22,24] However, the use of parametric methods can be difficult and restrictive for both practical and theoretical reasons. In fact, these methods are not general purpose but problem oriented, and a precise functional form is often difficult to be assumed. In addition, even when a certain functional form is chosen, e.g., a sum of lagged normals,[17] critical issues remain, e.g., the number of terms. Although parametric deconvolution has been intensively exploited to estimate the transport function, these and other critical issues, e.g., local minima in parameter optimization, have encouraged the use of nonparametric deconvolution approaches.[3,5,8,20] However, obtaining the transport function by nonparametric deconvolution, especially in the presence of recirculation, can be difficult. First of all, nonparametric deconvolution

cannot provide estimates at times greater than D_e. For instance, in our case, $D_e=45$, but, since the duration of $h(t)$ is greater than D_e, an estimate of the transport function up to infinity is needed in order to evaluate the left term of Eq. (5) correctly. Such a knowledge is also crucial for a correct calculation of the MTT by Eq. (2). Even when D_e is large enough, accurate estimates of the MTT are difficult to provide since, because of ill conditioning, the tail of the estimated transport function can be artifactually oscillatory and can present a maximum transit time, which is "determined by the duration of the data collection period rather than the duration of the actual transport function." [8]

Our approach will thus be as follows. First, we will develop a nonparametric deconvolution method to provide an estimate of $h(t)$ for $t \leq D_e$. Then, we will use a model to extrapolate $h(t)$ up to infinity.

The Deconvolution Method to Estimate $h(t)$ for Times not Greater than the Experiment Duration. To estimate $h(t)$ for $t \leq D_e$, we will use a recently presented nonparametric deconvolution method.[11,25] For certain aspects, this method can be seen as an evolution of the widely known Phillips–Tikhonov regularization approach,[21,27] which was applied to the estimation of transport functions in Refs. 3, 5, and 8 under the assumption of uniform sampling.

Let us denote by $y=[y_1,y_2,y_3,\ldots,y_n]^T$ the n-dimension vector of the (noisy) output IDC data. Having assumed that measurement error is additive, we have

$$y=z+v, \tag{6}$$

where $z=[z_1,z_2,z_3,\ldots,z_n]^T$ is the vector whose components are the n (noise-free) samples of $z(t)$ of Eq. (1) on Ω_{sv} and $v=[v_1,v_2,v_3,\ldots,v_n]^T$ is the n-dimension vector of the measurement errors, independent, and with zero mean. The covariance matrix of v is diagonal and its ith entry is assumed to be equal to $(CVy_i)^2$, with CV=0.06.

The function $h(t)$ is, in general, a smooth function since it represents the probability density function of the transit times of the indicator through the organ. In order to exploit this *a priori* information, we calculate the estimate $\hat{h}(t)$ by solving the following optimization problem:

$$\min_{\hat{h}(t)} \int_0^\infty \{\hat{h}^{(2)}(t)\}^2\, dt, \tag{7}$$

subject to

$$\|y-\hat{z}\|_{B^{-1}}=(y-\hat{z})^T B^{-1}(y-\hat{z})=\xi, \tag{8}$$

where $\hat{h}^{(2)}(t)$ denotes the second time derivative of $\hat{h}(t)$, $\hat{z}$ is the n-dimension vector obtained by considering $\hat{h}*u$, i.e., the "reconvolution," on Ω_{sv}, B is a matrix of weights (typically, the covariance matrix of v), and ξ is a real non-negative number (the symbol "$*$" denotes convolution).

The problem of Eqs. (7) and (8) is defined by having in mind the following rationale: Equation (8) fixes a distance, denoted by ξ, between the (noisy) data vector y and the model predictions vector $\hat{z}$. [Thanks to the presence of B^{-1} in Eq. (8), the adherence to each datum can be weighted differently.] Due to the ill posedness of the deconvolution problem, there is an infinite number of continuous-time functions $\hat{h}(t)$ having the selected distance ξ between their convolution with $u(t)$ and the data. By virtue of Eq. (7), the algorithm selects the one having a minimum second time derivative energy, i.e., the smoothest $\hat{h}(t)$ according to Ref. 21. The smaller is ξ, the more the adherence to the data vector y will be pursued.

To solve the problem [Eqs. (7) and (8)], a continuous-time function should be obtained from discrete data. In order to numerically provide an approximate solution, let us consider two grids, in keeping with Refs. 10 and 25. The first grid, denoted by $\Omega_{sv}=\{t_1,t_2,\ldots,t_k,\ldots,t_n\}$, is simply the (experimental) vein sampling grid. The second grid, denoted by $\Omega_v=\{T_1,T_2,\ldots,T_k,\ldots,T_N\}$, is an arbitrary grid much finer than Ω_{sv} ($N \gg n$). The grid Ω_v does not need to have any experimental counterpart and, for such a reason, it is called the virtual grid. Here, we define $\Omega_v=\{0.1,0.2,\ldots,45\}$ (note that $\Omega_{sv} \subset \Omega_v$).

Let $z_v(T_k)$ denote the (noise-free) output at virtual sampling times T_k. The grid Ω_v is so fine that the true but unknown $h(t)$ can be well approximated by a piecewise constant within each time interval of it, so that, from Eq. (1), it holds,

$$z_v(T_k)=\int_0^{T_k} u(T_k-\tau)h(\tau)\,d\tau$$
$$=\sum_{i=1}^{k} h(T_i)\int_{T_{i-1}}^{T_i} u(T_k-\tau)\,d\tau, \tag{9}$$

where $T_0=0$. In matrix-vector notation, we have

$$z_v=U_v h, \tag{10}$$

where z_v and h are the vectors of the output IDC and of the transport function samples considered on the virtual grid Ω_v, and U_v is a $N \times N$ lower triangular matrix whose entries are

$$U_v(k,i)=\int_{T_{i-1}}^{T_i} u(T_k-\tau)d\tau, \quad k\leq i. \tag{11}$$

Note that, since the virtual sampling is uniform, U_v is a square lower-triangular Toeplitz matrix, i.e., the elements of each diagonal of U_v are equal, so that it is determined by its first column. Times belonging to the virtual grid Ω_v but not present in the output grid Ω_{sv} do not correspond to sampled output data. We can regard them as (virtually) missing data. Denote by U the $n\times N$ matrix obtained by canceling from U_v those rows, which do not correspond to actually sampled data. U has a near-to-Toeplitz structure, meaning that it misses the rows deleted from the Toeplitz matrix U_v. The n-dimension vector y of Eq. (6) can thus be modeled as

$$y=z+v=Uh+v. \tag{12}$$

In this matrix-vector model, the N-dimension vector h is unknown. An estimate of vector h, say vector $\hat{h}$, can be obtained by solving

$$\min_{\hat{h}} \hat{h}^T Q^T Q\hat{h}, \tag{13}$$

subject to

$$\|y-U\hat{h}\|_{B^{-1}}=(y-U\hat{h})^T B^{-1}(y-U\hat{h})=\xi, \tag{14}$$

where Q is a N-dimension square lower-triangular Toeplitz matrix whose first column is $[1,-2,1,0,...,0]^T$, such that $Q\hat{h}$ is the vector of the second differences of $\hat{h}$ on Ω_v. The solution of the "finite-dimensional" problem given by Eqs. (13) and (14) approximates the solution of the "infinite-dimensional" problem given by Eqs. (7) and (8), and can be found by solving the optimization problem

$$\min_{\hat{h}}(y-U\hat{h})^T B^{-1}(y-U\hat{h})+\gamma\hat{h}^T Q^T Q\hat{h}, \tag{15}$$

where the real non-negative parameter γ is the inverse of the Lagrangian multiplier associated with ξ of Eq. (14). The closed-form solution of Eq. (15) is

$$\hat{h}=(U^T B^{-1}U+\gamma Q^T Q)^{-1}U^T B^{-1}y. \tag{16}$$

Readers familiar with the Phillips–Tikhonov regularization method will easily recognize the characteristic cost function of problem (15), made up of two terms: the first term gives the distance of the model predictions from the data; the second term gives a measure of the regularity of $\hat{h}$. The tuneable parameter γ [or the correspondent ξ of Eq. (14)] balances the relative importance of these two quantities. By raising γ, the cost of roughness of $\hat{h}$ increases, and matching the data vector y becomes relatively less important. For such a reason, γ is called the regularization parameter. Too large values of γ will lead to very smooth realizations of $\hat{u}$, which may be not able to explain the data (oversmoothing). Conversely, too small values of γ can lead to ill-conditioned estimates $\hat{h}$. To choose γ, several criteria have been proposed in the literature. Here, we will adopt the widely used *discrepancy* regularization criterion proposed in Ref. 28, which allows us to exploit the available knowledge on the measurement error variance, differently from, e.g., the generalized cross-validation criterion of Ref. 12. The discrepancy criterion suggests to adjust γ until the residual sum of the squares equals the sum of the measurement error variances. In our notation, γ must be tuned until $\mathrm{WRSS}=(y-U\hat{h})^T B^{-1}(y-U\hat{h})=n$, where WRSS denotes the weighted residual sum of squares.

Remark 1. To generate the entries of U given by Eq. (11), we used in place of $u(t)$ the linear interpolation of its raw samples. We also tried more sophisticated techniques, such as exponentials sums or cubic splines approximations, but we obtained estimates of h virtually identical to those provided by the simple linear interpolation method, at the cost of considerable extra modeling effort. A possible explanation of why this happens is that, in the solution of the problem we are dealing with, the deconvolution algorithm takes advantage from the fact that the input mostly consists of a large Dirac pulse, which renders the shape of the output IDC very similar to that of the transport function, especially in the first 10 min.

Remark 2. If the actual time course of $u(t)$ in Eq. (11) were known, the used discrepancy regularization criterion would be at risk of oversmoothing.[11,14] Here, the fact that the discrepancy criterion provides more smoothing than other criteria is welcome because of the presence, in addition to output IDC data noise, of a second source of error in Eq. (12), i.e., the errors on the entries of U. Of note is that, in order to avoid bias error to affect the initial sharp variations of the transport function, regularization was performed for $t>5$ min only. This is accomplished by infinitely weighting the adherence to the vein data for $t<5$, i.e., $B(i,i)=0$ if $t_i<5$, $t_i\in\Omega_{sv}$. As a consequence, the algorithm selects the smoothest function, which exactly describes the data for $t<5$ and has, at the same time, the prescribed distance ξ from the data for $t\geq 5$.

Remark 3. The solution of problem (15) can be efficiently obtained by employing the singular value decomposition strategy of Ref. 11, which, in order to further speed up calculations, can also exploit the Toeplitz structure of U and Q. Should "linear regularization" be not sufficient to obtain non-negative estimates because of high ill conditioning, one can employ the constrained conjugate gradient algorithm of Ref. 7.

Having fixed a trial value of F, the above deconvolution algorithm can provide an estimate of the transport function on Ω_v. Of note is that, for a finer and finer Ω_v, the estimate would converge to a time-continuous function.

Extrapolation of $\hat{h}(t)$ to Infinity and Estimation of F

The algorithm cannot estimate $h(t)$ for $t>D_e$, but this knowledge is crucial to assess if constraint (5) is satisfied. In fact, in our case, $\hat{h}$ for $t=D_e$ is small, but not small enough to neglect the contribution of the transport function for $t>D_e$ in the calculation of the integral of Eq. (5). There is, thus, the need of providing $\hat{h}(t)$ for $t>D_e$ also. Since the kinetics of the tracer are linear, it is expected that, for large t, the impulse response $h(t)$ decays with its slowest exponential,[6,19] i.e., the tail of the transport function can be described by a monoexponential model

$$\hat{h}_e(t)=Ae^{-\alpha t}, \tag{17}$$

whose parameters can be estimated from the samples of $\hat{h}(t)$ for $t\in[t_e,D_e]$ by nonlinear least squares,[6] with t_e ranging between 30 and 36, depending on the individual's deconvoluted transport function. Note that this exponential approximation of the transport function tail will also contrast possible oscillations to come into play in the estimation of MTT.

Having estimated the parameters of $\hat{h}_e(t)$, the area under $\hat{h}(t)$ can be computed, by the Eulero numerical integration method for $t<t_e$ and algebraically for $t>t_e$, to verify if constraint (5) is satisfied. Note that, for any trial value of F, if one accepts only those $\hat{h}_e(t)$, which fit well the tail of $\hat{h}$, the area under $\hat{h}(t)$ is monotonically increasing with F. Thus, for a certain trial value of F, if the area under $\hat{h}(t)$ is less than 1, F must be increased, otherwise it must be decreased.

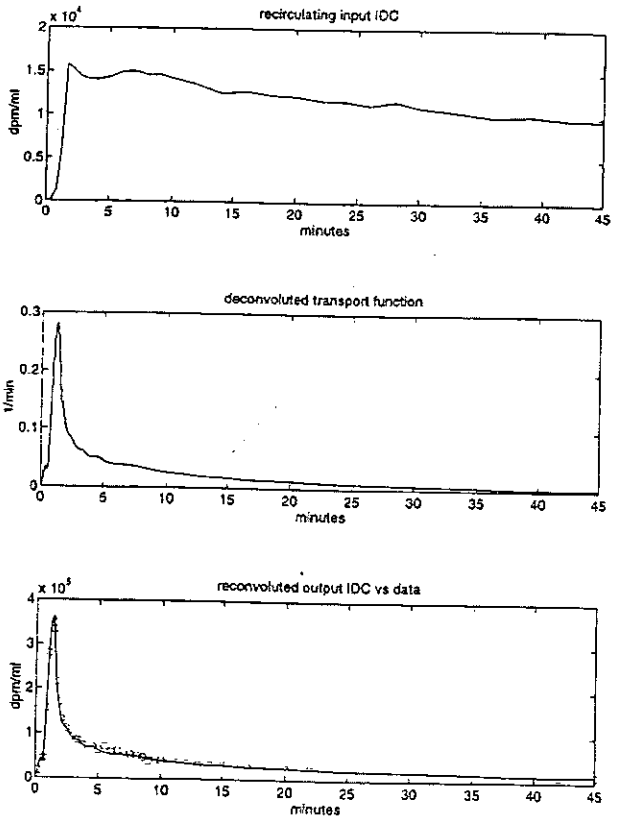

FIGURE 3. Estimation of the transport function by deconvolution in a representative subject (No. 4). *Top.* The recirculation input $u^R(t)$, obtained by first-order interpolation of the artery IDC samples of Fig. 1. *Middle.* Deconvoluted transport function $\hat{h}(t)$ for $t\in[0, 45]$ with $F=175$. *Bottom.* Reconvolution $\hat{z}(t)$ vs vein IDC samples.

Remark 4. The following alternate strategy would also be feasible. Having provided $\hat{h}(t)$ for $t\leq D_e$ for a trial value of F, one first computes the area under $\hat{h}(t)$ for $t\leq t_e$, say a_{dec}, and then defines $a_{\text{res}}=1-a_{\text{dec}}$. Having replaced A in model (17) with $a_{\text{res}}\alpha e^{\alpha t_e}$, the parameter α is estimated from the samples of $\hat{h}$ for $t\in[t_e,D_e]$. Since the area under $\hat{h}_e(t)$ for $t>t_e$ is, by construction, equal to a_{res}, $\hat{h}(t)$ satisfies Eq. (5) independently on the goodness of the trial value of F. The algorithm terminates if the selected F allows $\hat{h}_e(t)$ to fit well the samples of $\hat{h}(t)$ for $t\in[t_e,D_e]$, i.e., "white" residuals are produced; otherwise a different F is selected and the procedure is repeated. This strategy leads to results identical to those obtained with the previously presented technique. However, since the constraints on the parameters of $\hat{h}_e(t)$ makes Eq. (5) satisfied for any value of F, this strategy is much more demanding because an inspection of $\hat{h}_e(t)$ fit is required even for very wrong trial values of F.

RESULTS

Figure 3 shows the results for a representative study. The recirculation input $u^R(t)$, obtained by the first-order interpolation of the raw artery IDC samples of Fig. 1, is shown (top panel) together with the estimated transport function $\hat{h}(t)$ for $t\leq D_e$ computed by deconvolution with

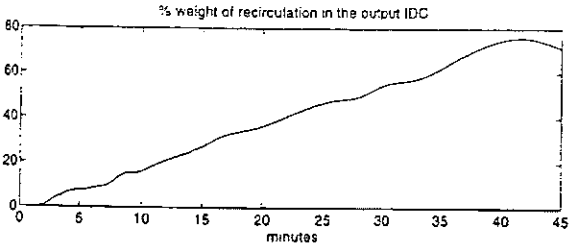

FIGURE 4. Extent of recirculation in the vein IDC in a representative subject (No. 4) calculated from Eq. (18).

$F=175$ (middle panel) and the convolution of $u(t)$ with $\hat{h}(t)$, i.e., the reconvolution profile $\hat{z}(t)$, against the vein IDC samples (bottom panel).

To assess the extent by which recirculation affects the vein data, it is useful to define the function

$$\hat{z}^r(t)=\frac{\hat{z}(t)-\frac{D}{F}\hat{h}(t)}{\hat{z}(t)}\times 100, \qquad (18)$$

whose numerator gives the difference between the model predictions of what is observable in the vein, i.e., $\hat{z}(t)$, and what would have been observed if recirculation did not occur, i.e., $(D/F)\times\hat{h}(t)$. Equation (18) thus gives the percent weight of recirculation in the vein IDC. It is easily understood that $\hat{z}^r(t)$ is an estimate of a function, which is expected to be monotonically increasing, and, for $t\to\infty$, to tend to the plateau value of 100. Figure 4 displays $\hat{z}^r(t)$ in the representative subject. Note that, for instance, 20% of the indicator concentration in the vein at $t=12$ is due to the presence of early recirculation, while at $t=45$, recirculation contributes to 80% of the datum.

Similar results have been obtained for all the other subjects.

Of note is that, in three/four subjects, the area under $\hat{h}(t)$ for $t>D_e$ resulted up to 0.08. In other words, there can be up to the 8% of probability that a particle leaves the ideally open-loop system for times greater than D_e. This indicates that extrapolation is here a necessity at variance, e.g., of Ref. 8, where the probability that transit times go beyond D_e was not significant and, in order to avoid oscillations in $\hat{h}$ to affect the estimation of MTT, the transport function tail was simply forced to zero when it was decreased down to 0.5% of the amplitude of its peak. Results also indicate that, in order to improve the robustness of the monoexponential model of the transport function tail in these subjects, and thus, of the MTT estimate, an increase of D_e, e.g., by 10 min, would be beneficial; in addition, more samples in the IDCs tails should be taken. The overall cost of the experiment would not increase with this improved sampling schedule since less data can be collected in the interval 8–25 min (see the simulation study below).

TABLE 1. Estimates of plasma flow, mean transit time, and extracellular volume.

Subject	F (ml/min)	MTT (min)	V (ml)
1	330	5.94	1960
2	240	10.24	2467
3	240	8.01	1923
4	175	11.01	1920
5	280	7.48	2096
6	190	8.19	1556
7	230	8.61	1982
8	135	10.13	1368
9	275	9.75	2684
10	225	7.12	1603
11	235	9.62	2262
12	215	10.68	2296
Mean±SD	230±51	8.89±1.58	2002±386

Having obtained $\hat{h}(t)$ from zero to infinity, the MTT can be calculated in a straightforward manner. Subsequently, the extracellular volume V can be computed by Eq. (3). Table 1 reports a summary of the results obtained in the 12 human subjects. The mean MTT, F, and V are, respectively, equal to 8.89 ± 1.58 min, 230 ± 51 ml/min, and 2002 ± 386 ml.

To assess reproducibility, the experimental protocol was repeated on a separate occasion in subjects Nos. 7, 8, 9, and 11 under the same conditions. A summary of the results together with their percent variations from the previous study are reported in Table 2.

The estimates of F, MTT, and V are reasonable. In fact, various direct measurement techniques[26] provided

TABLE 2. Estimates of plasma flow, mean transit time, and extracellular volume in the reproducibility study. Percentage variations from the previous study (Table 1).

Subject	F (ml/min)	ΔF%	MTT (min)	ΔMTT %	V (ml)	ΔV%
7	235	2	9.94	15	2338	17
8	155	14	10.74	6	1665	21
9	210	−23	11.41	17	2396	−10
11	225	−4	11.33	17	2550	12

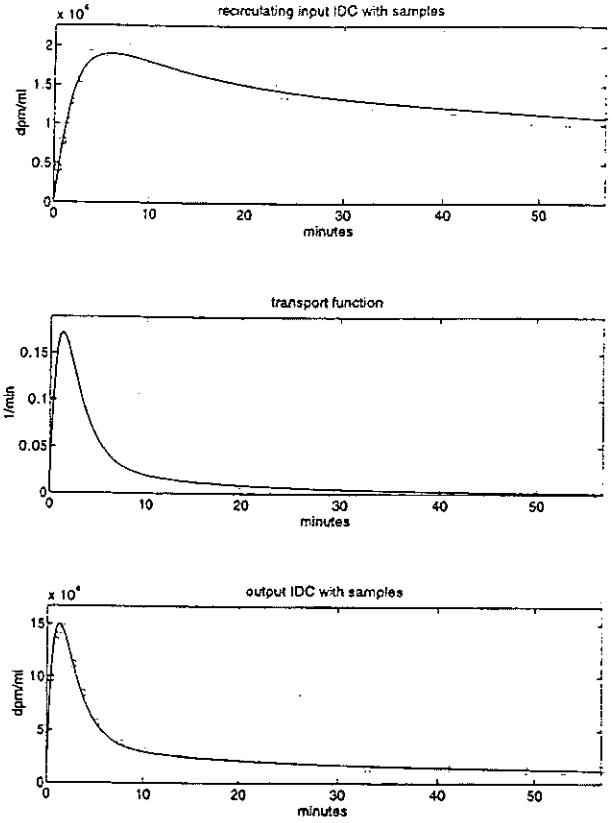

FIGURE 5. Simulation study. *Top.* True recirculating artery IDC (continuous line) with one noisy simulated data set (open bullets). *Middle.* True transport function $h(t)$ for $t \in [0, 57]$. *Bottom.* True vein IDC (continuous line) with one noisy simulated data set (open bullets).

blood flow values ranging from 150 to 500 ml/min. Thus, the mean plasma flow we obtain is within the expected range. In addition, since total leg volume in humans ranges from 5 to 10 l,[9] a mean extracellular volume around 2000 ml is in line with expectations.

MONTE CARLO SIMULATION

In this section, the accuracy and the precision of the method are assessed by a Monte Carlo study.

A functional expression was chosen for $u^R(t)$ and $h(t)$ (see the Appendix for details). The bolus contribution to $u(t)$ of Eq. (4) was given by $D = 2 \times 10^8$ and $F = 230$. The "true" MTT and V are 9.98 min and 2296 ml, respectively. 300 sets of simulated noisy samples of the IDCs were generated by assuming an additive measurement error, independent, and Gaussian with a constant CV equal to 6%. An improved sampling grid was chosen (see the Appendix), with D_e increased to 57 min, more samples in the IDC tails and less in the interval 8–25 min. One of the 300 simulated data sets is shown in Fig. 5 together with the true IDCs and transport function. Assuming F to be unknown, the method to recover the transport function was applied to the 300 simulated data sets.

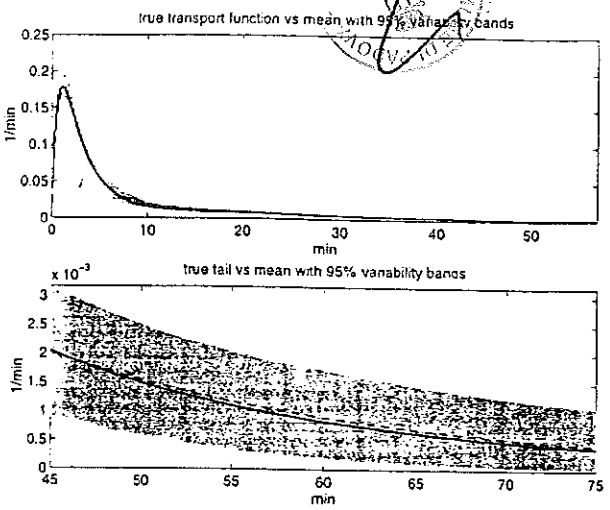

FIGURE 6. Transport function Monte Carlo results. *Top.* True $h(t)$ (dashed line), mean $\hat{h}(t)$ (continuous line) with 95% variability bands (shaded area) for $t \in [0, 57]$. *Bottom.* Tail of the true $h(t)$ (dashed line), mean of $\hat{h}_e(t)$ (continuous line) with 95% variability bands (shaded area).

Figure 6 (top panel) shows, for $t \in [0, D_e]$, the true $h(t)$ and the mean of the 300 estimates $\hat{h}(t)$ together with the 95% variability bands, i.e., the interval between the 2.5 and the 97.5 percentiles of the Monte Carlo distribution of the estimate at each time point. The average $\hat{h}(t)$ is (slightly) biased in the interval 5–15 min because of regularization.[15] As expected, the variability of $\hat{h}(t)$ is larger for $t < 5$, i.e., where smoothness is not weighted (see Remark 2). Figure 6 also shows (bottom panel), for $t \in [45,70]$, the tail of the true $h(t)$ and the mean of the 300 estimates $\hat{h}_e(t)$ together with their 95% variability bands.

In each Monte Carlo run, MTT, F, and V were also estimated. Figure 7 displays the histograms obtained from the 300 simulations. Average values with CV for MTT, F, and V are 9.82 (23%), 239 (6%), and 2361 (17%), respectively. Note that the mean MTT, F, and V are not significantly biased with respect to the "true" parameter values. The slight underestimation of MTT reflects the small bias of $\hat{h}(t)$ with respect to $h(t)$ in the interval around 10 min. Note that, since the estimates of F and MTT are somewhat correlated, the estimate of V is less dispersed than that of MTT.

Additional simulation studies (not shown) were also performed to assess if an extra modeling effort of approximating $u^R(t)$ with techniques more sophisticated than linear interpolation, e.g., splines, would be beneficial. No significant improvement was observed.

CONCLUSIONS

The transport function of an extracellular indicator through an organ, e.g., the human skeletal muscle of the leg, allows the computation of important physiological parameters, e.g., the mean transit time of the indicator from inlet to outlet and its distribution volume. The latter quantity is of particular interest because, under particular physiopathological conditions, it can significantly change due to recruitment of new tissue.

In the presence of recirculation, the estimation of the transport function is difficult because of both experimental and methodological problems. Here, in particular, since the plasma flow was not directly measured, the input IDC was not completely known and it was not possible to apply the methods available in the literature to recover the transport function.

To attack the problem, we developed a method which, starting from the input IDC model of Eq. (4), jointly estimates the transport function and the plasma flow. The method is based on a recently presented nonparametric deconvolution method and a monoexponential interpolation/extrapolation procedure, which approximates the tail of the transport function. The major advantage of the nonparametric approach to deconvolution lies in the fact that it does not require dealing with nontrivial problems such as system structure determination. The interpolation/extrapolation approach is parametric and has its basis on the linearity of the tracer kinetics; however, in order to avoid identifiability problems, a suitably designed sampling schedule and experiment duration is necessary. It is also worth noting that the input IDC could be modeled as in Eq. (4) only because the tracer bolus injection was very fast (about 1.5 s) with respect to the minimum transit time of the system (in our case, results predict that the probability that a transit time is less than 30 s is of the order of 1%): in well-perfused organs (where transit times may be very short), the validity of Eq. (4) can be critical.

The accuracy and the precision of the method were assessed by a Monte Carlo strategy. The good Monte Carlo results, together with the satisfactory reproducibility, encourage the use of the method presented in this paper for studying the transport of extracellular tracers in various physiopathological situations. For instance, studies with ^{3}H-mannitol can be carried out to assess if, in both normal and diabetic humans, the extracellular volume of the skeletal muscle is influenced by insulin.

ACKNOWLEDGMENTS

This work has been partially supported by a MURST grant "Bioingegneria dei Sistemi Metabolici e Cellulari." by National Institutes of Health Grant Nos. RR-11095, RR-02176, DK-42469, M01-RR-750-19, and DK-20542, and by a Veterans Affairs Merit Review grant.

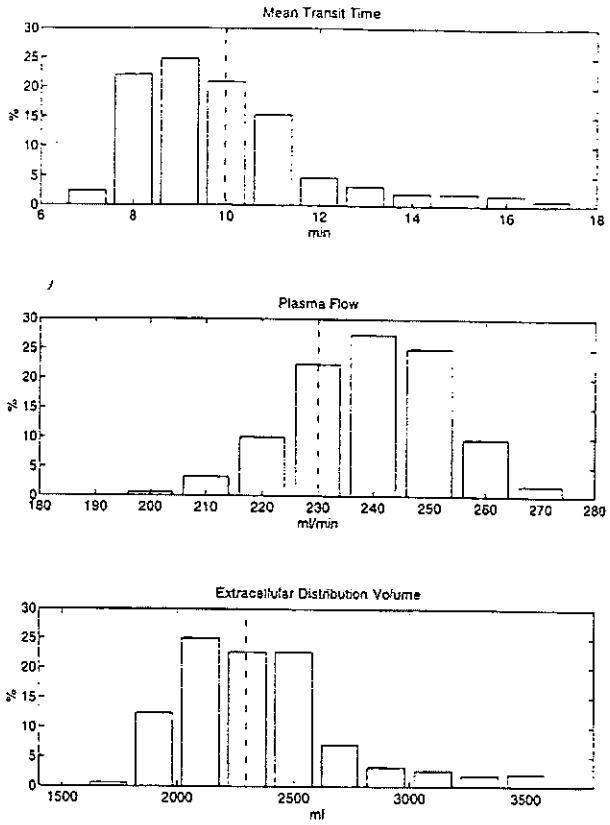

FIGURE 7. Monte Carlo frequency distribution of the parameters. *Top.* MTT. *Middle. F. Bottom. V.* Equally spaced bins are used in each panel. Dashed-dot lines denote true parameter values.

APPENDIX

In this appendix we report some details on the Monte Carlo study.

The recirculation input $u^R(t)$ is

$$u^R(t)=\sum_{i=1}^{4} B_i e^{-\beta_i t}+B_5 t^n e^{-\beta_5 t}. \qquad \text{(A1)}$$

$B_1=14{,}000$, $\beta_1=0.005$, $B_2=4000$, $\beta_2=0.05$, $B_3=6500$, $\beta_3=0.1$, $B_4=-(B_1+B_2+B_3)$, $\beta_4=0.5$, $B_5=1000$, $\beta_5=1.6$, and $n=4$.

The transport function is

$$h(t)=\sum_{i=1}^{5} A_i e^{-\alpha_i t}, \qquad \text{(A2)}$$

with $A_1 = 0.0173$, $A_2 = 0.0173$, $A_3 = 0.3468$, $A_4 = 0.6243$, $A_5 = -(A_1 + A_2 + A_3 + A_4)$, $\alpha_1 = 0.05$, $\alpha_2 = 0.1$, $\alpha_3 = 0.5$, $\alpha_4 = 1$, and $\alpha_5 = 1.2$.

The sampling grids are: $\Omega_{sv} = \Omega_{sa} = \{0.4, 0.8, 1.2, 1.6, 2.6, 3.6, 5, 7.6, 10, 14, 19, 24, 29, 33, 37, 41, 45, 49, 53, \text{and } 57\}$.

REFERENCES

[1] Baron, A., G. Brechtel-Hook, A. Johnson, and D. Hardin. Skeletal muscle blood flow. A possible link between insulin resistance and hypertension. *Hypertension* 21:129-135, 1993.

[2] Bassingthwaighte, J., F. Ackerman, and E. Wood. Applications of the lagged normal density curve as a model for arterial dilution curves. *Circ. Res.* 18:398–415, 1966.

[3] Bock, J., P. Deuflhard, A. Hoeft, H. Korb, G. Wolpers, J. Steinmann, and G. Hellige. Thermal recovery after passage of the pulmonary circulation assessed by deconvolution. *J. Appl. Physiol.* 64:1210–1216, 1988.

[4] Bonadonna, R., S. Del Prato, E. Bonora, M. P. Saccomani, G. Gulli, A. Natali, S. Frascerra, N. Pecori, E. Ferrannini, D. Bier, C. Cobelli, and R. De Fronzo. Roles of glucose transport and glucose phosphorylation in muscle insulin resistance of NIDDM. *Diabetes* 45:915–925, 1996.

[5] Bronikowsky, T., C. Dawson, and J. Linehan. Model-free deconvolution techniques for estimation of vascular transport functions. *Int. J. Bio-Med. Comput.* 14:411–429, 1983.

[6] Carson, E., C. Cobelli, and L. Finkelstein. The Mathematical Modeling of Metabolic and Endocrine Systems. New York: Wiley, 1983, p. 394.

[7] Commenges, D. The deconvolution problem: Fast algorithms including the preconditioned conjugate-gradient to compute a MAP estimator. *IEEE Trans. Autom. Control.* 29:229–243, 1984.

[8] Clough, A., D. Cui, J. Linehan, G. Krenz, C. Dawson, and M. Maron. Model-free numerical deconvolution of recirculating indicator concentration curves. *J. Appl. Physiol.* 74:1444–1453, 1993.

[9] Dela, F., J. J. Larsen, K. J. Mikines, T. Ploug, I. N. Petersen, and H. Galbo. Insulin-stimulated muscle glucose clearance in patients with NIDDM. Effects of one-legged physical training. *Diabetes* 44:1010–1020, 1995.

[10] De Nicolao, G., D. Liberati, and A. Sartorio. Deconvolution of infrequently sampled data for the estimation of growth hormone secretion. *IEEE Trans. Biomed. Eng.* 42:678–697, 1995.

[11] De Nicolao, G., G. Sparacino, and C. Cobelli. Nonparametric input estimation in physiological systems: Problems, methods, case studies. *Automatica* 33:851–870, 1997.

[12] Golub, G., M. Heath, and G. Wahba. Generalized cross-validation as a method for choosing a good ridge parameter. *Technometrics* 21:215–224, 1979.

[13] Grimm, D., J. Linehan, and C. Dawson. Longitudinal distribution of vascular resistance in the lung. *J. Appl. Physiol.* 43:1093–1101, 1977.

[14] Hall, P., and D. Titterington. Common structure of techniques for choosing smoothing parameters in regression problems. *J. R. Stat. Soc. Ser. B* 49:184–198, 1987.

[15] Hunt, B. R. Biased estimation for nonparametric identification of linear systems. *Math. Biosci.* 10:215–237, 1971.

[16] King, R., E. Deussen, G. Raymond, and J. Bassingthwaighte. A vascular transport operator. *Am. J. Physiol.* 265:H2196–H2208, 1993.

[17] Knopp, T., W. Dobbs, J. Greenleaf, and J. Bassingthwaighte. Transcoronary intravascular transport functions obtained via a stable deconvolution technique. *Adv. Biomed. Eng.* 4:44–59, 1976.

[18] Lasko, M., S. Edelman, G. Brechtel, and A. Baron. Impaired insulin mediated skeletal muscle blood flow in patients with non-insulin dependent diabetes mellitus. *Diabetes* 41:1076–1083, 1992.

[19] Lassen, N. A., and W. Pearl. Tracer Kinetic Methods in Medical Physiology. New York: Raven, 1979, p. 391.

[20] Nakai, M. Computation of transport function using multiple regression analysis. *Am. J. Physiol.* 240:H133–H144, 1981.

[21] Phillips, D. L. A technique for the numerical solution of certain integral equations of the first kind. *J. Assoc. Comput. Mach.* 9:97–101, 1962.

[22] Pollastri, A., M. Pistolesi, and C. Giuntini. A method for computing frequency functions from input–output vascular dilution curves. *J. Nucl. Med. Allied Sci.* 21:165–177, 1977.

[23] Saccomani, M. P., R. C. Bonadonna, D. M. Bier, R. A. DeFronzo, and C. Cobelli. A model to measure insulin effects on glucose transport and phosphorylation in muscle: A three-tracer study. *Am. J. Physiol.* 270:E170–E185, 1996.

[24] Schroder, T., U. Rosler, H. Hoeft, M. Scholz, J. Hering, and G. Hellege. Calculation of body transport function. *Phys. Med. Biol.* 37:2059–2069, 1992.

[25] Sparacino, G., and C. Cobelli. A stochastic deconvolution method to reconstruct insulin secretion rate after a glucose stimulus. *IEEE Trans. Biomed. Eng.* 43:512–529, 1996.

[26] Steinberg, H., H. Chaker, R. Leaming, A. Johnson, G. Brechtel, and A. Baron. Obesity/insulin resistance is associated with endothelial dysfunction. Implications for the syndrome of insulin resistance. *J. Clin. Invest.* 97:2601–2610, 1996.

[27] Tikhonov, A. N. Solution of incorrectly formulated problems and the regularization method. *Sov. Math. Dokl.* 4:1035–1038, 1963.

[28] Twomey, S. The application of numerical filtering to the solution of integral equations encountered in the indirect sensing measurements. *J. Franklin Inst.* 279:95–109, 1965.